Solid State Communications 252 (2017) 29–32

Contents lists available at ScienceDirect

Solid State Communications

journal homepage: www.elsevier.com/locate/ssc

Communication

High pressure structural and magnetic studies of $LaFe_{12}B_6$

L.V.B. Diop[a,b,*], O. Isnard[a,b], Z. Arnold[c], J.P. Itié[d], J. Kastil[a,b,c], J. Kamarad[c]

[a] Univ. Grenoble Alpes, Inst NEEL, F-38042 Grenoble, France
[b] CNRS, Inst NEEL, F-38042 Grenoble, France
[c] Institute of Physics AS CR v.v.i., Na Slovance 2, 182 21 Prague 8, Czech Republic
[d] Synchrotron SOLEIL, L'Orme des Merisiers Saint Aubin BP48, 91192 Gif-sur-Yvette Cedex, France

ARTICLE INFO

Keywords:
Magnetization
Itinerant-electron system
High pressure
Compressibility

ABSTRACT

The study of the structural and magnetic properties of $LaFe_{12}B_6$ under high pressure has been performed by combining angle-dispersive x-ray powder diffraction at room temperature up to 14 GPa and magnetization measurements up to 1 GPa. At ambient pressure, the itinerant-electron compound $LaFe_{12}B_6$ exhibits an antiferromagnetic ground state below T_N=36 K. It is demonstrated that the antiferromagnetic state can be transformed into a ferromagnetic state via a field-induced first-order metamagnetic transition accompanied with a large magnetic hysteresis. The x-ray diffraction measurements under pressure reveal that the ambient pressure crystal structure of $LaFe_{12}B_6$ is preserved up to 14 GPa with a decrease of the unit cell parameters. A compressibility value of κ=4.90 10^{-3} GPa^{-1} has been determined. The application of an external pressure leads also to the progressive decrease of the Néel temperature dT_N/dP=−4.5 K GPa^{-1}. In addition a large pressure effect on the critical field $\mu_O H_{cr}$ of the metamagnetic transition, $d\mu_O H_{cr}/dP$=24 T GPa^{-1}, was discovered. This clearly indicates the crucial role of volume effect on the itinerant-electron metamagnetic transition.

1. Introduction

The $RT_{12}B_6$ borides, where R is a rare-earth element or yttrium and T is a 3d transition metal (Co or Fe), adopt the rhombohedral $SrNi_{12}B_6$-type structure, space group $R\bar{3}m$ [1–3]. The transition metal atoms are located on two inequivalent crystal sites (18 g and 18 h) with the rare-earth and boron atoms occupying the 3a and 18 h sites, respectively. $RCo_{12}B_6$ systems are stable for essentially all of the rare-earths, they are ferro– (R=Y, La–Sm) or ferri– (R=Gd–Tm) magnets with a rather small average Co magnetic moment – 0.42 μ_B/Co in $YCo_{12}B_6$ – and low ordering temperatures T_C=134–162 K [4]. While $NdFe_{12}B_6$ was the first iron-based example of the $RT_{12}B_6$ series of compounds to be discovered [5], it is however metastable and $LaFe_{12}B_6$ is the unique stable iron-based member of the series [6,7]. The metastable ternary compound $NdFe_{12}B_6$ is ferromagnetic and undergoes an order-disorder magnetic transition at T_C=230 K [5]. $LaFe_{12}B_6$ compound is not only the unique stable $RFe_{12}B_6$ phase, along the rare-earth R series, but also presents unique magnetic behaviour including an unusual amplitude-modulated magnetic structure, particularly small Fe magnetic moment in the ground state, multicritical point in the magnetic phase diagram and remarkably low ordering temperature T_N=36 K [8]. This ordering temperature is much smaller compared to the $RCo_{12}B_6$ intermetallic compounds and an order of magnitude smaller than the ordering temperature of any iron rich R-Fe binary system. ^{57}Fe Mössbauer spectroscopy and high field magnetization (up to 35 T) studies on $LaFe_{12-x}Co_xB_6$ [6] and $La_{1-x}Gd_xFe_{12}B_6$ [7] have shown that $LaFe_{12}B_6$ is a compound with Fe moments close to magnetic instability. This unstable character of the Fe moment has been confirmed by tight-binding calculations which further pointed out that the magnetic moment of Fe on the 18 h site is more sensitive to its environment [9,10]. The itinerant-electron character of the magnetism of this $LaFe_{12}B_6$ compound has been established and its remarkable magnetic properties revealed [8,11,14]. $LaFe_{12}B_6$ is an antiferromagnet exhibiting an exceptionally large field-induced metamagnetic transition in a wide range of temperature including below and above the Néel temperature T_N [7,8,11–14]. Interestingly, peculiar giant metamagnetic transitions consisting of a succession of steep magnetization jumps separated by plateaus were most recently discovered at very low temperatures (typically below 8 K) in $LaFe_{12}B_6$ [8,12–14]. Below a certain crossover temperature the metamagnetic transition transforms from a spectacular smooth to ultrasharp step-like transitions. Yet another striking result found in $LaFe_{12}B_6$ is the observation of huge spontaneous jump in magnetization where both the temperature and the magnetic field are constant. It has been demonstrated that this giant spontaneous magnetization jump takes place after a very long silent time known as the "incubation time" [12].

* Corresponding author at: Univ. Grenoble Alpes, Inst NEEL, F-38042 Grenoble, France.
E-mail address: leopoldbirane@gmail.com (L.V.B. Diop).

http://dx.doi.org/10.1016/j.ssc.2017.01.010
Received 18 November 2016; Received in revised form 9 January 2017; Accepted 13 January 2017
Available online 14 January 2017
0038-1098/

Magnetic properties of itinerant-electron systems strongly depend on the electronic band structure. Thus the magnetic properties of such system are expected to be sensitive to pressure because the application of pressure results in an increase of the band width, affecting the density-of-states DOS at the Fermi energy E_F. In spite of its exceptional magnetic behaviour, too few attentions have been paid in $LaFe_{12}B_6$ intermetallic compound, the influence of pressure on the itinerant-electron metamagnetic transition, on the ordering temperature and on the crystal unit cell remains unknown so far. In order to get information about the role of volume in the structural and magnetic properties of $LaFe_{12}B_6$ we have investigated the external pressure effect by means of synchrotron x-ray diffraction and magnetization measurements.

2. Methods

Polycrystalline $LaFe_{12}B_6$ sample was prepared by melting high-purity starting elements (Alfa Aesar, La—99.9%, Fe—99.99%, B—99.9%) in a high frequency induction furnace under a purified argon gas atmosphere as reported in Refs. 8,12–14. A slight excess of La was used in order to avoid the presence of α-Fe as an impurity phase. To promote homogeneity, the $LaFe_{12}B_6$ button was melted several times, then wrapped in a Ta foil and subsequently annealed at 900 °C for three weeks in evacuated quartz tube. The synthesized material was characterized by chemical analysis, as well as by x-ray diffraction performed on powder diffractometer in reflection mode with the Bragg-Brentano geometry, using Co-Kα radiation, with scan step 0.02° and angular 2θ range from 20° to 90°.

High-pressure synchrotron x-ray diffraction measurements were carried out at the PSICHÉ beamline, Synchrotron SOLEIL, France, at room temperature in angle-dispersive mode (λ=0.37384 Å). Diamond anvil cell (DAC) was used up to 14 GPa. Steel gaskets were preindented and holes were drilled at the center of the indentation. Sample, along with ruby chips, were placed at the center of the drilled cavity. A mixture of methanol and ethanol was used as pressure transmitting medium. Pressure was measured both before and after each measurement using the ruby fluorescence technique. To improve the powder statistic, the sample was rotated ± 5° during the exposure. Two-dimensional diffraction images were collected using a MAR detector and the resulting diffraction data were azimuthally integrated with the FIT2D program [15]. The patterns were analyzed by Rietveld refinements using the software package FullProf [16].

Magnetization measurements under pressure up to 1 GPa were performed at magnetic fields up to 7 T in the temperature range from 2 K to 100 K in a SQUID magnetometer (Quantum Design Co.) using a miniature CuBe hydrostatic pressure cell. The cell was filled with a mixture of mineral oils as a pressure transmitting medium. The pressure was determined at low temperatures using the known pressure dependence of the critical temperature of the superconducting state of the Pb sensor placed inside the cell [17].

3. Results and discussion

In order to probe the pressure dependence of the crystal structure, angle-dispersive x-ray powder diffraction patterns have been collected at room temperature for various applied pressures up to 14 GPa. Selected diffraction patterns in the compression cycle are compared in Fig. 1. The synthesized $LaFe_{12}B_6$ sample was found to be mainly single phase according to the x-ray diffraction investigation. A careful look at the diffractograms indicates the presence of residual traces of the binary Fe_2B compound as minority impurity phase. The analysis of the diffractograms confirms the $R\bar{3}m$ space group symmetry for the studied $LaFe_{12}B_6$ compound. The diffraction patterns under pressures show that the trigonal symmetry of the atomic arrangement remains unaltered within the investigated pressure range. The crystal structure of $LaFe_{12}B_6$ is stable up to the highest applied pressure. As can be seen from Fig. 1, the diffraction peaks are shifted to a higher angle due to the reduction of the unit cell volume.

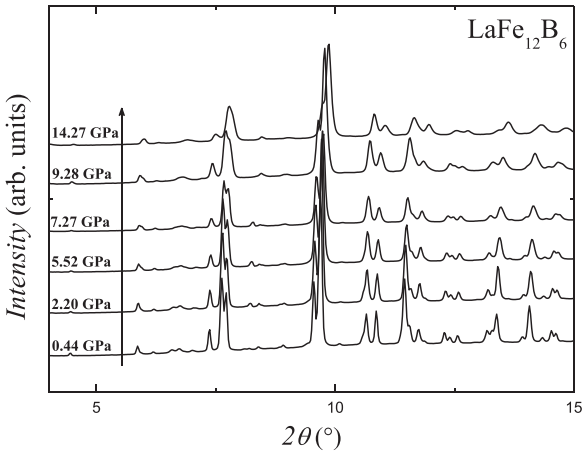

Fig. 1. X-ray diffraction patterns recorded at room temperature for $LaFe_{12}B_6$ at different applied pressures (λ=0.37384 Å).

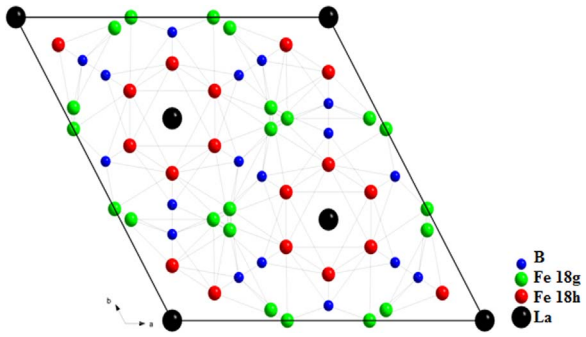

Fig. 2. Crystal structure of $LaFe_{12}B_6$.

The refined cell parameters at ambient pressure for $LaFe_{12}B_6$ are a=9.631(5) Å and c=7.612(1) Å values in good agreement with earlier reported studies [6]. The corresponding crystal structure is depicted in Fig. 2. The unit cell is composed of 3 formula units. The La atoms (3a Wyckoff site) have an axial symmetry ($\bar{3}$m) and a local environment which is made of 24 atoms, 6 of which are B ones, 12 Fe(18 g) type and 6 are Fe(18 h) ones. The local environment of Fe(18 g) atoms consists of 3 Fe(18 g) neighbours, 4 Fe(18 h) neighbours, 4 B neighbours and 2 La neighbours. The Fe(18 h) position is also surrounded by 13 near neighbours, but here one finds only one La neighbour, 4 Fe located at 18 g, 5 Fe(18 h) neighbours and 3 B neighbours. The B atoms have 8 near neighbours: 4 Fe at position 18 g, 3 Fe(18 h) and 1 La atom.

A Rietveld refinement of the diffraction pattern taken at 1 GPa is shown in Fig. 3 and the resulting parameters are given in Table 1. The extracted lattice parameters (a and c) values are plotted in Fig. 4 as a function of pressure. The a and c lattice parameters decrease linearly upon compression, and values of da/dP=−1.44 10^{-2} Å GPa^{-1} and dc/dP=−1.15 10^{-2} Å GPa^{-1} are obtained. This indicates an anisotropic shrinkage of the unit cell with a larger compression in the basal plane. The pressure dependence of the cell volume is displayed in Fig. 5. The observed pressure dependence of the cell volume was fitted with the third-order Birch-Murnaghan equation of state [19], where K_0' was fixed at 4. The performed fit yielded V_0=611.43 $Å^3$ for the zero-pressure cell volume and K_0=204 GPa for the bulk modulus. For comparison purposes we note that, $TiFe_2$ and $La(Fe_{0.88}Si_{0.14})_{13}$ present a bulk modulus value of 201 GPa and 125 GPa, respectively [20,21]. The bulk modulus of $LaFe_{12}B_6$ is 1.6 times larger than that of $La(Fe_{0.88}Si_{0.14})_{13}$.

Fig. 6 shows the temperature dependence of the magnetization of $LaFe_{12}B_6$ in a magnetic field of 2 T at various applied pressures. The magnetization was measured upon heating after zero-field cooling of

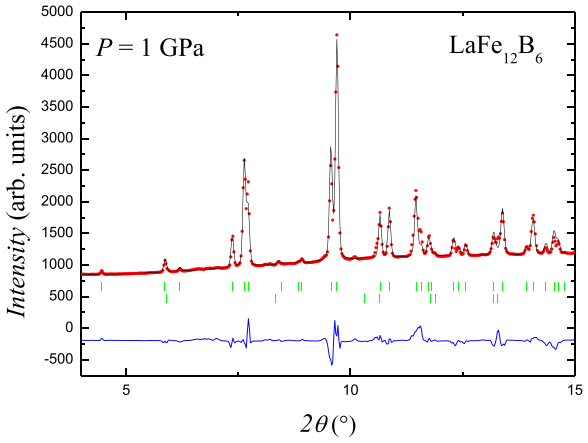

Fig. 3. Refinement of the x-ray diffraction pattern of $LaFe_{12}B_6$ at 1 GPa (λ=0.37384 Å). The top row of Bragg markers is for the $LaFe_{12}B_6$ majority phase. The second row is corresponding to the minority Fe_2B phase.

Table 1
Rietveld refinement results and reliability factors obtained from the analysis of the diffraction pattern taken at 1 GPa for $LaFe_{12}B_6$.

a=9.622 (4); c=7.603 (3) Å; R_{Bragg}=3.88%; R_{wp}=5.4%; R_p=7.2%; R_{exp}=2.36%			
	Fe (18 g)	Fe (18 h)	B (18 h)
x	0.370(3)	0.424(2)	0.483(3)
z	0.5	0.037(5)	0.286(2)

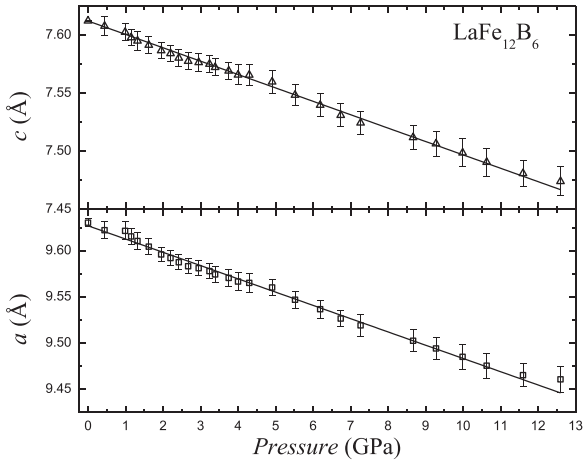

Fig. 4. Lattice parameters of $LaFe_{12}B_6$ as a function of pressure. The solid lines correspond to linear fit.

the sample. The ambient pressure thermomagnetic curve displays a peak at 36 K. Such peak is distinctive in antiferromagnets and reflects the magnetic phase transition from the antiferromagnetic (AFM) to the paramagnetic (PM) state. The peak position is denoted as the Néel temperature T_N. The order-disorder magnetic transition temperature, T_N=36 K found here at ambient pressure is in good agreement with earlier reported studies on the physical properties of $LaFe_{12}B_6$ by magnetization measurements [6–8,11–14], neutron powder diffraction [8], Mössbauer spectroscopy [6,11] or specific heat measurements [11]. Such magnetic ordering temperature is particularly low and unusual for an iron-rich intermetallic phase. From Fig. 6, one can clearly observe that both the magnetization and T_N are reduced by the application of external pressure. The magnetization and the ordering temperature show a negative pressure dependence.

The pressure dependence of the Néel temperature T_N, as derived from isofield magnetization curves, is illustrated in Fig. 7. The pressure

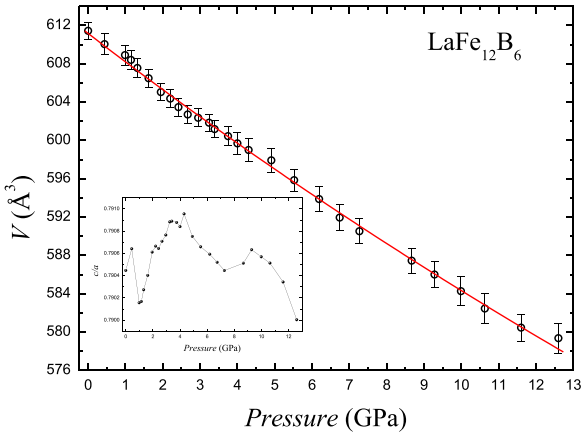

Fig. 5. Unit cell volume of $LaFe_{12}B_6$ as a function of pressure. The solid red line represents the third-order Birch-Murnaghan fit for the data. Inset of the figure shows the c/a ratio.

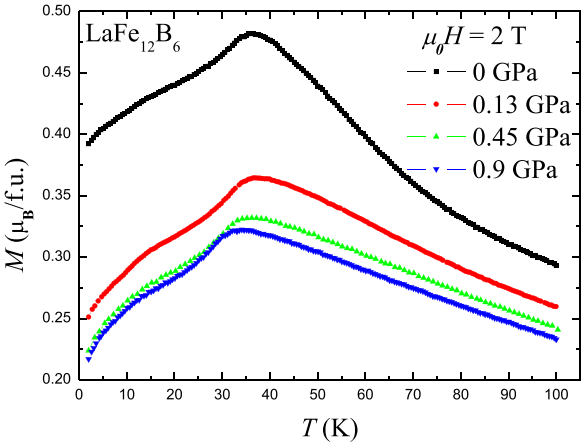

Fig. 6. Temperature dependence of the magnetization recorded for several applied pressures on $LaFe_{12}B_6$.

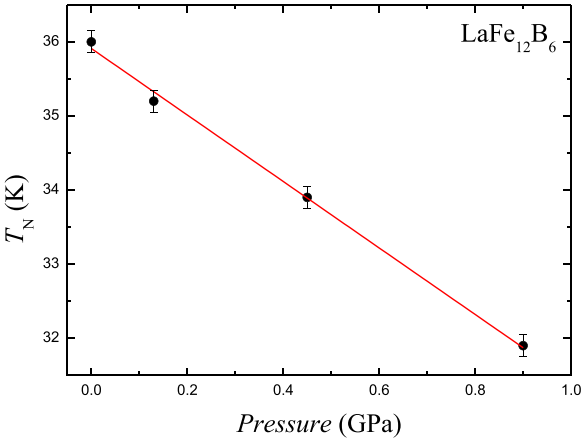

Fig. 7. Pressure dependence of the Néel temperature T_N of $LaFe_{12}B_6$.

induced decrease of T_N is linear in the used pressure range and value of the pressure slope, dT_N/dP=−4.5 K GPa^{-1} is obtained. The observed pressure effect on the Néel temperature T_N of $LaFe_{12}B_6$ system is quite comparable to the recently reported pressure induced change on the Curie temperature of isostructural compound $LaCo_{12}B_6$, dT_C/dP=−4.7 K GPa^{-1} [18]. This similar value of the pressure dependence of their ordering temperature is rather surprising if one keep in mind the different nature of the magnetic order in the two compounds AFM versus FM for $LaFe_{12}B_6$ and $LaCo_{12}B_6$ respectively as well as the large

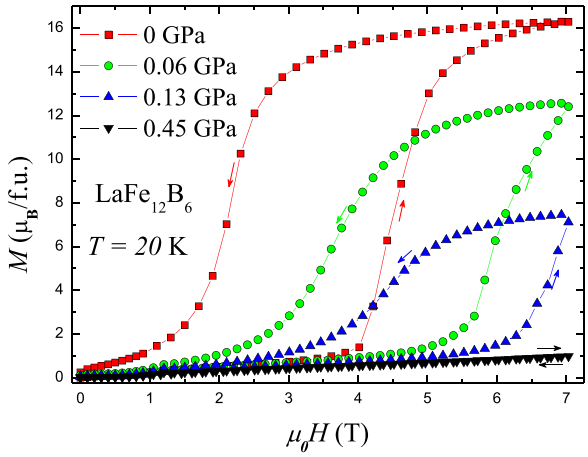

Fig. 8. Isothermal magnetization curves recorded at 20 K under various applied pressures for $LaFe_{12}B_6$.

difference in their ordering temperature 36 K against 160 K. Taking dT_N/dP=−4.5 K GPa^{-1} for $LaFe_{12}B_6$ system, the critical pressure for the disappearance of the antiferromagnetic order is estimated to be 8 GPa by a linear extrapolation to T_N=0 K.

As demonstrated in our recent papers [8,12–14], at finite temperatures, both AFM and PM states can be transformed into a ferromagnetic (FM) state via a field-induced transition. In order to facilitate discussion of the pressure effect on the transition field $\mu_0 H_{cr}$, isothermal magnetization measurements under hydrostatic pressure were performed. These magnetization isotherms allow also to clarify the magnetic state at different temperatures, magnetic fields and pressures. The initial magnetization data and the corresponding field-decreasing branches at 20 K under several applied pressures are presented in Fig. 8. The arrows indicate the magnetic field directions in which the measurements have been performed. At ambient pressure, $LaFe_{12}B_6$ exhibits a metamagnetic transition from the AFM to the field-induced FM phase accompanied with a large magnetic hysteresis of 2.5 T. The observed hysteresis in the magnetization process upon increasing and decreasing magnetic fields confirms the first-order nature of the field-induced AFM-FM phase transition. Fig. 8 indicates clearly a large sensitivity of $LaFe_{12}B_6$ to the application of pressure, one can notice a strong shift of the metamagnetic transition to higher magnetic field upon increasing the applied pressure. The observed reduction of the largest magnetization value reached at 7 T does not necessarily indicate a reduced saturation magnetization but rather that the 7 T used are not enough to saturate the $LaFe_{12}B_6$ system under high pressure. The critical field $\mu_0 H_{cr}$ of the metamagnetic transition is determined as the maximum of the first derivative of the magnetization isotherms. The critical field is correlated with the free energy difference between the AFM and FM states. The critical field drastically increases with increasing pressure with an initial slope $d\mu_0 H_{cr}/dP$=24 T GPa^{-1}, reaching our maximum attainable field of 7 T around 0.11 GPa. This large pressure sensitivity indicates that the free energy difference between the AFM and FM state in the present system is significantly influenced by the external pressure through magnetovolume coupling. In $LaFe_{12}B_6$ application of hydrostatic pressure enhances the stability of the AFM phase. In this case the effect of pressure is opposite to the action of the magnetic field: applied magnetic field favors the larger magnetization FM phase.

4. Conclusion

The high-pressure x-ray diffraction study has shown that the $LaFe_{12}B_6$ crystal structure is stable at least up to 14 GPa. Upon compression, the unit cell shrinks continuously with a larger compression in the basal plane. Our investigation has demonstrated a large sensitivity of the itinerant-electron metamagnetic transition to external pressure. In $LaFe_{12}B_6$ a slight change of volume induces a drastic change of the critical field of the metamagnetic transition, indicating the crucial role of volume effect on the electronic properties of such compound.

Acknowledgements

We gratefully acknowledge SOLEIL for the access to the synchrotron radiation facility (Proposal No. 20130584). The authors warmly acknowledge the financial support of CNRS-ASRT cooperation program and the Project 15-03777S GA CR. J. Kastil also thanks the French government for PhD grant under the scope of the EIFFEL n. 784044F.

References

[1] K. Niihara, S. Yajima, Chem. Lett. **1** (1972) 875.
[2] Yu. B. Kuz'ma, G.V. Chernyak, N.F. Chaban, Dopov. Akad. Nauk. Ukr. RSR Ser. A **12** (1981) 80.
[3] W. Jung, D. Quentmeier, Z. Kristallogr. **151** (1980) 121.
[4] M. Mittag, M. Rosenberg, K.H.J. Buschow, J. Magn. Magn. Mater. **82** (1989) 109.
[5] K.H.J. Buschow, D.B. de Mooij, H.M. van Noort, J. Less-Common Met. **125** (1986) 135.
[6] M. Rosenberg, T. Sinnemann, M. Mittag, K.H.J. Buschow, J. Alloys Compd. **182** (1992) 145.
[7] Q.A. Li, C.H. de Groot, F.R. de Boer, K.H.J. Buschow, J. Alloys Compd. **256** (1997) 82.
[8] L.V.B. Diop, O. Isnard, J. Rodriguez-Carjaval, Phys. Rev. B **93** (2016) 014440.
[9] G.I. Miletic, Z. Blazina, J. Magn. Magn. Mater. **323** (2011) 2340.
[10] G.I. Miletic, Z. Blazina, J. Alloys Compd. **430** (2007) 9.
[11] S. Fujieda, K. Fukamichi, S. Suzuki, J. Magn. Magn. Mater. **421** (2017) 403.
[12] L.V.B. Diop, O. Isnard, Appl. Phys. Lett. **108** (2016) 132401.
[13] L.V.B. Diop, O. Isnard, J. Appl. Phys. **119** (2016) 213904.
[14] L.V.B. Diop, O. Isnard, J. Alloys Compd. **688** (2016) 953.
[15] A.P. Hammersley, S.O. Svensson, M. Hanfland, A.N. Fitch, D. Hausermann, High Press. Res. **14** (1996) 235.
[16] J. Rodrıguez-Carvajal, Physica B **192** (1993) 55.
[17] J. Kamarad, Z. Machatova, Z. Arnold, Rev. Sci. Instrum. **75** (2004) 5022.
[18] L.V.B. Diop, Z. Arnold, O. Isnard, J. Kamarad, J. Alloys Compd. **593** (2014) 163.
[19] F. Birch, Phys. Rev. **71** (1947) 809.
[20] Y. Wu, X. Wu, S. Qin, K. Yang, J. Alloys Compd. **558** (2013) 160.
[21] E. Valiev, I. Berger, V. Voronin, V. Glazkov, A. Kaloyan, K. Podurets, Phys. Solid State **56** (2014) 14.